Journal of Membrane Science 392–393 (2012) 88–94

Contents lists available at SciVerse ScienceDirect

Journal of Membrane Science

journal homepage: www.elsevier.com/locate/memsci

Transport of liquid water through Nafion membranes

Qiongjuan Duan[a], Huaping Wang[a], Jay Benziger[b,*]

[a] College of Material Science and Engineering, State Key Laboratory for Modification of Chemical Fibers and Polymer Materials, Donghua University, Shanghai 201620, PR China
[b] Chemical and Biological Engineering, Princeton University, Princeton, NJ 08544 USA

ARTICLE INFO

Article history:
Received 3 October 2011
Received in revised form 4 December 2011
Accepted 5 December 2011
Available online 13 December 2011

Keywords:
Hydraulic permeation
Nafion
Pore network

ABSTRACT

The flux of liquid water through Nafion membranes of different thickness and equivalent weight was measured as a function of hydrostatic pressure and temperature. Hydraulic water transport across Nafion membranes increases with temperature and equivalent weight of the Nafion. Hydraulic permeability increases with temperature due to both decreased water viscosity and increased hydrophilic volume fraction. Convective flow from the applied hydrostatic water pressure is an order of magnitude greater than the estimated diffusive water flux associated with the water activity gradient. Water sorption and hydraulic permeability data predict a hydrophilic pore network with hydrophilic domains 2.5 nm in diameter spaced 5.5 nm apart. The pore network structure from water sorption and hydraulic permeability are consistent with the spacing between hydrophilic domains observed with small angle X-ray scattering experiments.

1. Introduction

Water transport through Nafion membranes is essential for the successful operation of Polymer Electrolyte Membrane (PEM) Fuel Cells. Water made at the cathode catalyst layer, situated between the PEM and the porous cathode gas diffusion layer (GDL) must be removed. Depending on the resistances to transport, water can either flow through the porous GDL to the cathode gas flow channel or flow through the PEM to the anode catalyst layer, anode GDL and anode gas flow channel. Water is transported through the PEM both by diffusion, due to an activity gradient, and by convection, due to a hydraulic pressure difference between the cathode and anode. In a typical PEM fuel cell there might be a pressure difference of 0.1 MPa between the cathode and the anode. There has been many studies of water transport by diffusion through PEMs over the past several years [1–16]. In contrast there has been only a few reports of convective water transport through PEMs [2,5,17]. We report here results for water uptake and convective water transport through the PEM Nafion.

Nafion is the most common and popular PEM employed in fuel cells. It is a perfluorosulfonic acid made by copolymerization of tetrafluoroethylene and a perfluorovinyl ether terminated with a sulfonyl fluoride [18]. After polymerization the sulfonyl fluoride is hydrolyzed and ion exchanged to produce the perfluorosulfonic acid. Nafion microphase separates into hydrophilic domains comprised of sulfonic acid groups and sorbed water that is surrounded by a hydrophobic matrix of tetrafluoroethylene and perfluoro ethers. Water sorption swells the hydrophilic domains providing paths for proton transport and water diffusion [19,20]. We expect that convective water transport driven by a hydraulic pressure will also be through the hydrophilic domains. Several versions of Nafion membranes are available that differ by membrane thickness, density of sulfonic acid groups and the capping groups on the ends of the polymer chains. We anticipate that the hydraulic permeation of water will correlate with the hydrophilic volume fraction and inversely with the membrane thickness. Recent studies characterizing the diffusive transport of water across Nafion membranes with different equivalent weights (EW = mass of polymer/mole of $SO_3^-X^+$) and different membrane thickness have shown that interfacial transport at the vapor/membrane interface can limit water transport across thin Nafion membranes, but there is negligible transport resistance at the liquid/membrane interface [1,2,4,20,21].

PEM fuel cells are often operated with pressure differences between the anode and cathode; water can be transported across the membrane by diffusion driven by a water activity difference and by convection driven by a hydraulic pressure difference. Two recent papers have reported hydraulic permeability of water through Nafion was small and increased with temperature [2,4]. Kientiz et al. examined Nafion 212 and 211 and suggested that hydraulic permeability was small relative to diffusive transport of water [2]. We have extended the previous studies to compare water permeation through Nafion membranes with different thickness, different equivalent weight and different capping groups. The results show that hydraulic permeability increases with temperature and volume fraction of water in the membrane. The hydraulic radius of the water channels and their spacing were determined from

* Corresponding author. Tel.: +1 609 258 5416.
E-mail address: benziger@princeton.edu (J. Benziger).

0376-7388/$ – see front matter © 2011 Elsevier B.V. All rights reserved.
doi:10.1016/j.memsci.2011.12.004

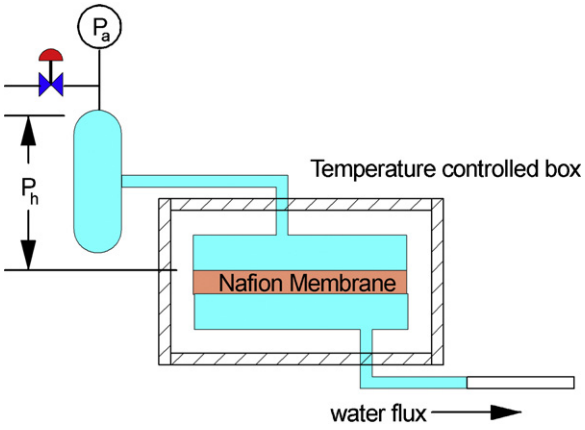

Fig. 1. Schematic of flow cell for water convection through Nafion membranes.

measurements of water volume fraction and water flow rate in a porous network. The distance between hydrophilic domains was ~5.5 nm in agreement with the characteristic length observed by scattering experiments [18].

2. Experimental

2.1. Flow experiments

Liquid water flow rates were measured with the permeation cell shown schematically in Fig. 1. Two polycarbonate blocks were machined with plenums 2.5 cm diameter × 1.25 cm deep. The blocks were bolted together with a polymer membrane placed between the two plenums. A support cross was fitted in the low pressure plenum to limit deflection of the polymer membrane. Water was fed to one plenum from a pressurized reservoir. The hydrostatic pressure from the height of the water reservoir above the membrane and the applied gas pressure were combined to give a total hydraulic pressure. The outlet from the second plenum went into a 1.6 mm ID tygon tube. The water flow rate across the membrane was determined from the distance the water moved through the tygon tube as a function of time. Water flow rates were measured at a fixed hydraulic pressure for a period of 2–3 h to obtain steady state flow rates. Flow rates were measured for both increasing and decreasing pressure changes. The permeation cell was placed inside an insulated heated box where the temperature was controlled.

2.2. Membrane preparation and treatment

All membranes were treated by boiling in 3% H_2O_2 for 1 h, rinsing in boiling deionized water for 20 min, boiling in 1 M H_2SO_4 for an hour and finally rinsing again in boiling deionized water for 30 min. Commercial extruded Nafion 115, Nafion 1110, Nafion 1035 and Nafion 212 were obtained from Ion Power (New Castle DE) and treated as outlined above. Nafion 115 and Nafion 1110 are both equivalent weight 1100 with dry thicknesses 127 and 254 μm, respectively. Nafion 212 is equivalent weight 1100 with a dry thickness of 51 μm. Nafion 212 has a different capping group on the polymer chain than Nafion 115 and Nafion 1110. Nafion 1035 is equivalent weight 1000 with a dry membrane thickness of 89 μm.

2.3. SAXS sample preparation

Small angle X-ray scattering was carried out on samples of Nafion 1110 equilibrated with water vapor and liquid water at room temperature and a sample placed in boiling water. The membranes were placed in a sealed sample cell constructed from two copper plates with mica windows and a Viton gasket between them. Membrane water contents, λ, were determined gravimetrically on samples having the same treatment as those being mounted in the SAXS cell.

The sample cell was placed in the path of the X-ray beam. In order to minimize membrane water loss during the data collection, helium gas was used in the flight tube rather than a vacuum. The 1.54 Å Cu-Kα X-rays were generated by a Philips XRG-3000 sealed tube generator source. The beam was slit collimated and the scattering was detected by an Anton-Paar compact Kratky camera equipped with a Braun OED-50M detector. Samples were run at room temperature for 10 min. Empty beam scattering, sample transmittance, and detector response were corrected for in the data analysis. The data reduction and desmearing procedures are described in detail by Register [22]. The invariant scattering intensity (q^2I) is plotted as a function of scattering angle or distance and the Bragg spacing is determined by the location of the peak in scattering intensity.

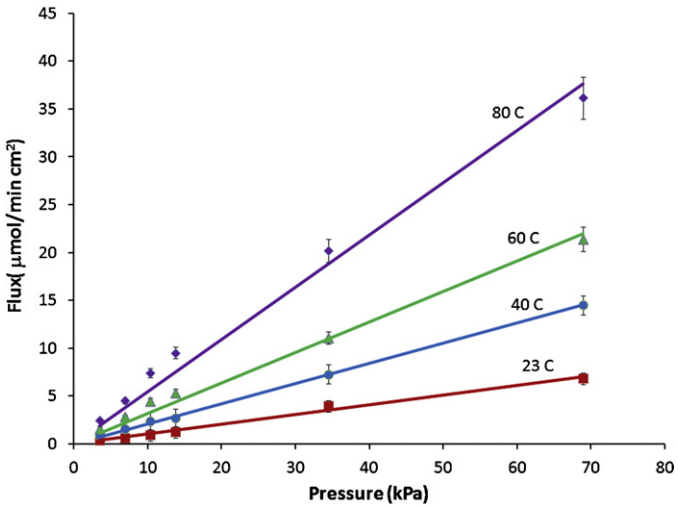

Fig. 2. Water flux through Nafion 115 membranes at different temperatures.

2.4. Water uptake

The equilibrium water uptake was measured as a function of water pressure at different temperatures using an isometric system [19,23]. A PEM is placed in a fixed volume container. The PEM sample was evacuated to below 1 Pa (<0.01 mbar) at 80 °C to remove all the water from the membrane. The pressure container was then cooled to the desired temperature under vacuum. The valve to the vacuum line was shut off and aliquots of water are injected into the pressure vessel and allowed to equilibrate with the Nafion. The resulting pressure is equal to the partial pressure of water. The difference between the quantity of water injected and the water in the gas phase is equal to the amount of water absorbed by the Nafion. Saturation was evident when the injection of a liquid aliquot did not cause any change in the pressure.

3. Results

The water fluxes as functions of applied hydraulic pressure for Nafion 115 at room temperature (~23 °C), 40, 60 and 80 °C are shown in Fig. 2. Data for different Nafion membranes, N115, N1110, N1035 and N212 at room temperature are shown in Fig. 3. These data are all well represented by a linear increase of water flux with applied hydraulic pressure. Table 1 summarizes the slope of the

Table 1
Nafion membrane hydraulic permeabilities and water sorption.

Membrane (EW)	T (°C)	μ (Pa s)	t_m (μm)	k_w ($cm^2 \times 10^{16}$)	λ_{sat} = #H_2O/SO_3
N115 (1100)	23	.100	127	3.75	21 ± 2
N115 (1100)	40	.065	127	5.04	22 ± 2
N115 (1100)	60	.047	127	5.49	24 ± 2
N115 (1100)	80	.035	127	7.13	25 ± 2
N1110 (1100)	23	.100	254	3.90	21 ± 2
N1035 (1000)	23	.100	89	5.77	21 ± 2
N212 (1100)	23	.100	51	4.09	21 ± 2

water flux (Q_w) vs. pressure (ΔP) for the different samples and different temperatures. Membrane permeabilities (k_w), defined by Eq. (1), were calculated from the flux data and are given in Table 1. The membrane permeability is expected to be independent of water viscosity, μ, and membrane thickness, t_m.

$$Q_w = \frac{k_w}{\mu t_m} \Delta P \quad (1)$$

The results indicate that the three membranes with the 1100 equivalent weight, N115, N1110 and N212, all had similar permeabilities circa 4×10^{-16} cm^2 at 23 °C. N1035, with an equivalent weight of 1000, had permeability about 40% greater than the 1100 EW Nafion. The permeability of N115 membranes increased with temperature. Since k_w corrects for the viscosity change with temperature, the data show that the permeability increased with temperature.

The saturation uptake of water into the Nafion membranes (reported as λ = number of water molecules sorbed per sulfonate group) are shown in Table 1. The saturation water volume increased modestly with increasing temperature. The saturation water volume at 23 °C was also larger for the 1000 EW Nafion (N1035) than the 1100 EW Nafion. (Even though λ was the same for N115 and N1035 the water volume fraction is larger for N1035 because the density of sulfonic acid groups is greater for N1035.)

Small angle X-ray scattering results for four different Nafion 1110 samples are shown in Fig. 4. More detailed studies can be found in a number of sources [18,24–27]. The purpose of Fig. 4 is to highlight the characteristic scattering length of ~5 nm for Nafion samples with absorbed water. There is no evidence of any scattering in the nm range for proton exchanged Nafion membranes without absorbed water. The other three samples correspond to water absorption at saturation conditions: saturated vapor at room temperature, saturated liquid at room temperature and saturated liquid at 100 °C. The SAXS results for 1100 EW Nafion indicate a small increase in water sorption between saturated vapor and liquid, and an additional small increase between saturated liquid at 20 °C and 100 °C. The characteristic scattering length increases slightly with increased water content in the membrane.

4. Discussion

The mechanisms of water transport in Nafion and structure of the "water channels" have been a source of intense interest over the past 25 years. Modeling efforts have examined different contributions of water sorption and transport including diffusion and convection. Eikerling and co-workers have considered various driving forces for convection including external pressure gradient, capillary pressure, osmotic pressure, and elastic forces associated with membrane deformation [28–31]. Experiments have lagged behind the modeling efforts for water transport and only recently have experimental results been published that provide details of transport resistances [1,4,5,10,20,32,33], mechanical properties [34,35] and water profiles [36–39] as functions of water activity and temperature. These recent experimental results can be compared with previous modeling efforts to improve the understanding of structure–property relationships in Nafion.

Water permeation, water sorption and SAXS studies of water in Nafion have been reported in the literature [18]. It is well established that water sorption in Nafion is accompanied by a strong scattering peak with a characteristic distance of ~5 nm. Water diffusion increases with water content in Nafion. However, there has been minimal quantitative connections between the structure of Nafion determined by scattering experiments and transport rates. We explore here the consistency of convective water transport through Nafion and the structure of the hydrophilic domains determined from scattering experiments. It will be shown that convective water transport coupled with water sorption predicts water

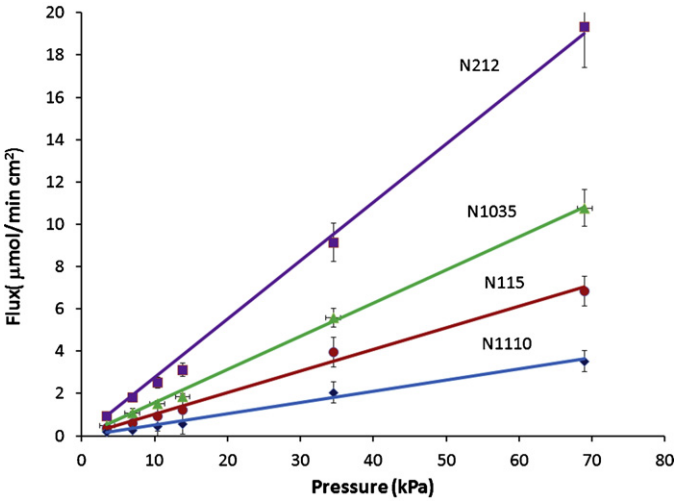

Fig. 3. Water flux through different Nafion Membranes at 23 °C.

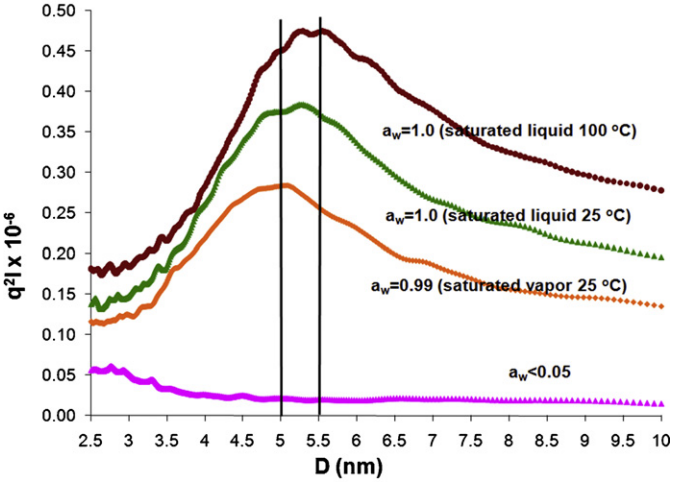

Fig. 4. Small angle X-ray scattering of Nafion 1110 membranes in saturated vapor, room temperature saturated liquid and saturated liquid at 100 °C.

is convected through a hydrophilic "channel" network consisting of 2.5 nm diameter water channels spaced 5.5 nm apart; this structure shows quantitative agreement with the results from SAXS.

4.1. Effect of temperature and equivalent weight on hydraulic permeability

Two recent papers have reported measurements of pressure driven water convection through Nafion. Weber and collaborators from Toyota reported permeability coefficients for Nafion 211 and Nafion 212 [2]. Their values for 1100 EW Nafion is in the range of $1–8 \times 10^{-16}$ cm^2 very close to those reported here at 60 and 80 °C. The permeability they measured at 25 °C was 4 times smaller than the value we report. Holdcroft and co-workers also measured hydraulic water permeability through Nafion 212 [4,5,21]. They also obtained values circa 10^{-16} cm^2 similar to those reported here. These recent values are almost 100 times less than earlier values reported by Bernaradi and Verbrugge [17]. We suspect there were some difficulties with those early experiments.

Hydraulic permeabilities at 23 °C were almost the same for N115, N1110 and N212, all of which have an equivalent weight of 1100. These three membranes also sorbed the same number of water molecules per sulfonic acid groups ($\lambda = 21 H_2O/SO_3$ at 23 °C). The hydraulic permeability of N1035, with EW 1000, is greater than the permeability of the 1100 EW Nafion membranes.

Our results, as well as those of Kientiz et al. and Adachi et al., found that the hydraulic permeability increased with temperature. In all three studies the water flux increased more than that predicted by the decrease of water viscosity with temperature, indicating that the hydraulic permeability increased with temperature. Results in Table 1 also show that the number of water molecules sorbed per sulfonic acid group increased with temperature, indicating that the volume fraction of water in Nafion increased with increasing temperature. The increase in hydraulic permeability with temperature and equivalent weight is greater than expected from the increased volume fraction of water. The water volume fraction, φ_w, given in Eq. (2) changes by almost 10% while the hydraulic permeability increased by 50–80%. This difference suggests there may be structural changes to the hydrophilic domains with increased water sorption beyond simple volume expansion.

$$\varphi_w = \frac{(\rho_{Nafion}/EW)\lambda V_w}{1 + (\rho_{Nafion}/EW)\lambda V_w} \quad (2)$$

4.2. Hydraulic permeation vs. pervaporation

The recent paper by Kientiz et al. compared the water fluxes from liquid/vapor pervaporation and liquid/liquid hydraulic permeation. They observed that the liquid/vapor pervaporation fluxes were significantly greater than the liquid/liquid hydraulic permeation fluxes. Kientiz et al. suggested that hydraulic permeation could be neglected relative to the pervaporation if there was an activity gradient [2]. Adachi et al. also made similar observations [4]. In our liquid/vapor permeation experiments in our labs we also observed larger pervaporation water fluxes than the convective water fluxes we report here [1,20,32]. Is hydraulic permeation important to water transport in Nafion?

Water transport across Nafion membranes is essential to both membrane humidifiers and PEM fuel cells. The water activity differences across the membrane are quite different in fuel cells compared to membrane humidifiers. Nafion membrane humidifiers operate as pervaporation cells with a small hydrostatic pressure difference (<10 kPa) but large relative humidity difference across the membrane [40–42]. In contrast, fuel cells have saturated liquid/gas streams at both sides of the membrane throughout most of the fuel cell; there is a negligible relative humidity difference, but a substantial hydrostatic pressure difference (~100 kPa) between the anode and cathode.

Benziger and co-workers, and Monroe et al. concluded that interfacial water transport at the membrane vapor interface is the principal resistance to water transport in pervaporation systems [1,8,20]. Because the limiting transport resistance is at the vapor/membrane interface, the water activity in the membrane is nearly constant across the membrane, approximately equal to the liquid water activity, as shown by Eq. (3), where k_m is a function of temperature.

$$(Q_{pervaporation}) = k_m(a_w^{membrane} - a_w^{vapor}) \approx k_m(a_w^{liquid} - a_w^{vapor}) \quad (3)$$

Saturated liquid activity is unity ($a_w^{saturated\ liquid} = 1$). The activity correction for a pressurized liquid is given by the Poynting correction shown in Eq. (4) (assuming that liquid water is incompressible over the pressures of interest).

$$a_w = a_w(P_w^{sat}) + \exp\left[\int_{P_w^{sat}}^{P} \frac{\bar{V}_w}{RT}\, dP\right] = 1 + \exp\left[\frac{(P - P_w^{sat})\bar{V}_w}{RT}\right]$$

$$\approx 1 + \frac{(P - P_w^{sat})\bar{V}_w}{RT} \quad (4)$$

The activity correction to pressurized water at 100 °C from saturation (0.1 MPa) to 1 MPa pressure (10 bar) is ~0.001. Hence, we conclude that at low to moderate differential pressures no measureable change to the water pervaporation flux is expected. This is consistent with pressurized pervaporation experiments by Kientiz et al. and Adachi et al. (We did similar experiments. Initially we observed a small change in the steady state flux for pressurized pervaporation through Nafion. However, when we followed the flux dynamically we discovered the change in flux was due to bowing of the membrane due to the pressure differential, which increased the interfacial area.)

There is no convective water flux across the membrane/vapor interface. Since interfacial transport at the vapor/membrane interface is the limiting resistance to pervaporation, any contribution to water transport by hydraulic permeation in the membrane will increase the water concentration at the membrane/vapor interface and reduce the already small water activity gradient across the membrane.

When liquid water is at both membrane surfaces the interfacial transport resistances are negligible. Unless there is a pressure (or temperature) gradient across the membrane there is no driving force for water transport. A differential pressure across the membrane will drive water transport by diffusion and hydraulic permeation. Diffusive permeation is driven by the water activity gradient across the membrane. The activity difference for pressurized liquid water on both sides of the membrane is given by the Poynting correction shown in Eq. (5).

$$\Delta a_w = \exp\left[\int_{P_{anode}}^{P_{cathode}} \left[\frac{\bar{V}_w}{RT}\right] dP\right] = \exp\left[\frac{(P_{anode} - P_{cathode})\bar{V}_w}{RT}\right]$$

$$\approx \frac{(P_{anode} - P_{cathode})\bar{V}_w}{RT} \quad (5)$$

The diffusive water flux ($Q_{w,diffusive}$) associated with the hydrostatic pressure difference across the membrane of thickness t_m, is given by Eq. (6); where D_w is the diffusion coefficient of water and c_w is the concentration of water in the membrane ($c_w = \lambda N_{SO_3} = \lambda \rho_{Nafion}/EW$ where N_{SO_3} is the density of sulfonic acid groups in Nafion). Diffusion coefficients for 1100 EW Nafion were reported by Zhao et al. [20]; $D_w(a_w = 1) \approx 5 \times 10^{-6}$ cm^2 s^{-1}.

$$Q_{w,diffusive} \approx D_w c_{w,mem} \frac{\Delta a_w}{t_m} = \frac{D_w \lambda N_{SO_3}}{t_m} \frac{(P_{anode} - P_{cathode})\bar{V}_w}{RT} \quad (6)$$

The ratio of the diffusive flux (Eq. (6)) to the convective flux (Eq. (1)) with liquid present on both sides of the membrane is given by Eq. (7).

$$\frac{Q_{\text{diffusive}}}{Q_{\text{convective}}} = \frac{D_w \lambda N_{SO_3} \mu \bar{V}_w}{RTk_w} \approx 3 \times 10^{-2} \quad (7)$$

When water is present at both sides of the Nafion membrane the diffusive flux from an applied pressure is only a small fraction of the hydraulic flux (~3%). In PEM fuel cells when the anode and cathode gas streams are both fully humidified the transport of water across Nafion membranes will be dominated by hydraulic permeation.

4.3. Water removal from the catalyst layer: through the membrane or through the GDL?

Water is produced at the cathode catalyst layer. The vapor is saturated in the cathode flow channel. There is no water activity gradient to drive diffusion from the cathode catalyst layer to the cathode gas flow channel, so liquid water will accumulate in the catalyst layer and build up a hydrostatic pressure. The water pressure will increase until the water pushes through either the membrane or the cathode gas diffusion layer. The pressure required to push water through the Nafion membrane depends on the current density of the fuel cell. The hydrostatic pressure to remove the water by transport through the membrane is found by equating the water flux through the membrane to the water production. The hydrostatic pressure differential to force the water through the membrane at typical fuel cell current densities would be very large (equation 8).

$$\Delta P = \frac{j/2F}{k_w/\mu t_m} \approx 1\,\text{MPa}, \quad j = 1\,\text{A/cm}^2 \quad (8)$$

The hydraulic pressure to force water through the membrane can be compared to the pressure to force liquid water through the GDL. Benziger and co-workers previously measured liquid water permeation through GDL materials [43]. There is a minimum pressure for liquid water penetration into the largest pores of the GDL of ~10 kPa. Above the penetration pressure the permeation coefficient through the GDL is $\sim 10^{-12}$ cm^2, which is much greater than $k_w \sim 10^{-16}$ cm^2 for permeation through the membrane. This simple calculation shows that most of the water formed at the cathode will be transported through the GDL to the cathode gas flow channel.

4.4. The hydrophilic pore network

Nafion consists of hydrophilic sulfonic acid groups dispersed in a hydrophobic matrix of tetrafluoroethylene and perfluoroalkyl ethers [18,24,44–53]. The sulfonic acid groups sorb water swelling the hydrophilic network through which water and protons are transported. The microphase separated structure of Nafion is analogous to a porous medium where water may be transported through a convoluted hydrophilic pore structure. Gierke proposed a pore structure with spherical hydrophilic clusters of sulfonic acid groups and water that are connected by narrow hydrophilic channels [44]. More refinements to the Gierke model have been proposed over the past 30 years based primarily on results from Small Angle X-ray scattering and Small Angle Neutron scattering [18]. Those results have shown that there is a characteristic scattering distance of ~5 nm that appears when water is sorbed in Nafion [24,27,48–51]. Most studies have associated that distance with the spacing between hydrophilic clusters in the Nafion [24,48,49,54]; however, some studies have suggested that the scattering peak corresponds to the size of the hydrophilic clusters [55,56].

Transport properties can also provide structural information about Nafion. Wu et al. have recently shown that there is a critical hydrophilic volume fraction (φ) threshold of 0.1 in 1100 EW Nafion for the hydrophilic domains to percolate through the hydrophobic matrix [19]. Above the critical threshold, proton conductivity increases quadratically with the hydrophilic volume fraction; $\sigma_{H^+} \sim (\varphi - \varphi_c)^2$. Zhao et al. have shown that water diffusion in Nafion also increases quadratically with the hydrophilic volume fraction; $D_w \sim \varphi^2$ [20]. Zhao also showed that tortuosity, τ, of the hydrophilic domains decreases dramatically with water volume fraction from $\tau \sim 20$ at $\varphi_w = 0.02$ to $\tau \sim 2$ at $\varphi_w \sim 0.1$.

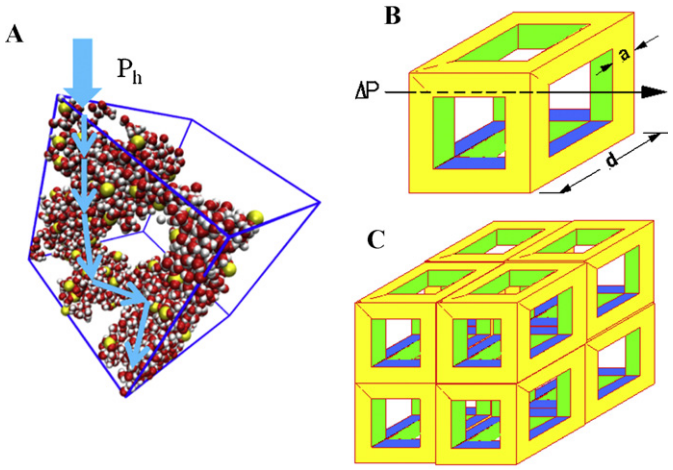

Fig. 5. Cell model for hydrophilic network structure. (A) This is the structure of Nafion predicted by molecular dynamics with $\lambda = 15H_2O/SO_3$. Only the water and sulfonic acid groups are shown. The voids are occupied by the TFE backbone and PFEA side chains. (B) A unit cell of a simplified model for Nafion assuming a geometrically regular structure. The hydrophilic domains are the struts and the voids are the hydrophobic domains. The hydraulic radius for water transport is given by a, and d is the spacing between hydrophilic domains. (C) The connection of unit cells to make a bicontinuous channel network.

The convection of water through Nafion can also serve as a probe to its structure. The hydrophilic domains form a network through which water flows. The water flux depends on the size and density of the hydrophilic channels. Fig. 5A shows molecular dynamics results from Daly for the hydrophilic phase separated domains for 1100 EW Nafion with $\lambda = 15H_2O/SO_3$ [57]. The hydrophilic domains form a channel network. A simplified model of the channel network in Nafion is illustrated in Fig. 5. This model is greatly simplified, assuming regularly spaced uniform channels. The utility of the model is to make quantitative predictions of flow rates through Nafion.

The microphase separated structure is approximated by a regular array of unit cells consisting of struts and cavities. The struts and cavities of the unit cell represent Nafion's phase separated structure. The volume fractions of the struts and cavities are characterized by two quantities: a = characteristic dimension of the hydrophilic channel (e.g. hydrodynamic radius), and d = characteristic distance between hydrophilic channels. The volume fraction of the struts, representing water sorbed into the hydrophilic channels is related to the two quantities a and d by Eq. (9). (One could imagine the hydrophilic and hydrophobic phases switched. Because the model is symmetric the results are independent of whether one assumed the hydrophilic phases consisted of the struts between vertices or the central voids.)

$$\varphi = 12\left(\frac{a}{d}\right)^2 - 16\left(\frac{a}{d}\right)^3 \quad (9)$$

The quadratic term in Eq. (9) is the volume of non-intersecting channels; the cubic term in Eq. (9) accounts for the overlapping volumes of channels going in different directions.

When a hydraulic pressure is applied it will cause water to flow in the direction of the pressure gradient; the applied pressure must

Table 2
Pore network parameters for liquid water flow in Nafion.

Membrane	T (°C)	φ_w	$[2k_w\tau]^{1/2}$ (nm)	a (nm)	d (nm)
N115	23	0.404 ± 0.03	0.27	1.12 ± 0.15	5.14 ± 0.2
N115	40	0.36 ± 0.03	0.32	1.26 ± 0.15	5.69 ± 0.2
N115	60	0.37 ± 0.03	0.33	1.24 ± 0.15	5.43 ± 0.2
N115	80	0.39 ± 0.03	0.38	1.38 ± 0.15	5.94 ± 0.2
N1110	23	0.34 ± 0.03	0.27	1.14 ± 0.15	5.25 ± 0.2
N1035	23	0.38 ± 0.03	0.34	1.28 ± 0.15	5.57 ± 0.2
N212	23	0.35 ± 0.03	0.28	1.17 ± 0.15	5.37 ± 0.2

overcome the viscous drag with the walls of the channels. The flow rate as a function of pressure drop may be approximated by Poiseuille flow (Eq. (10)), where laminar flow in uniform square channels with hydraulic radius r_h is assumed.

$$Q_{w,pore} = (2r_h)^2 \left[\frac{r_h^2}{8\mu}\frac{\Delta P}{L_{pore}}\right] \tag{10}$$

The total water flow for channels spaced at a distance d apart is given by Eq. (11). To account for distortions of the real pore network from the idealized model the effective length of the channels is given by the membrane thickness multiplied by a tortuosity factor, τ.

$$Q_w = \frac{(2r_h)^2}{d^2}\left[\frac{r_h^2}{8\mu}\frac{\Delta P}{L_{pore}}\right] = \left[\frac{r_h^4}{d^2}\right]\left[\frac{\Delta P}{2\tau\mu t_m}\right] \tag{11}$$

Eqs. (10) and (11) assume that the Poiseuille flow description of liquid flow through cylindrical channels can be extended to more complex geometries, this assumption has been validated for both gas and liquid flow through porous materials, leading to the commonly employed Kozeny equation for flow through porous media [58].

The hydraulic radius accounts for the volume available for flow divided by interfacial area over which the shear forces are exerted, as given by Eq. (12). The hydrophilic volume is the volume fraction of water sorbed into the polymer membrane, given by Eq. (2).

$$r_h = \frac{\text{hydrophilic volume/unit volume}}{\text{interfacial area/unit volume}} = \frac{\varphi_w}{\alpha_{int}} \tag{12}$$

The interfacial area between the hydrophilic domains and the hydrophobic matrix is not directly accessible for measurement. However, the interfacial area is related to the hydrophilic network parameters a and d, and is given by Eq. (13). Eq. (13) only includes the interfacial area of the struts in the direction of flow.

$$\alpha_{int} = 24a(d-2a) \tag{13}$$

The hydraulic radius can also be expressed as a function of the hydrophilic network parameters as given by Eq. (14).

$$r_h = \frac{3ad-4a^2}{3(d-2a)} \tag{14}$$

Eqs. (2) and (11)–(14) can be combined to determine a and d as functions of the experimentally measured and water volume fraction (φ_w) and water flow rate (Q_w).

The water volume fractions were determined from water sorption data and the results are listed in Table 2. From Eqs. (1) and (11) the experimental permeability can be related to the hydraulic radius and spacing between pores.

$$\frac{r_h^4}{d^2} = [2k_w\tau] \tag{15}$$

Assuming $\tau = 2$ from the measurements of Zhao et al. [20] values of a and d were determined for each membrane at the different temperatures using Eqs. (9) and (15); the results are summarized in Table 2.

The results indicate that the spacing between hydrophilic domains, d, ranges from 5 to 6 nm, increasing with water volume fraction. Those values agree with the characteristic distance observed from scattering experiments (e.g. see Fig. 4). The hydrophilic channel diameter, $d_{channel} = 2a$, is approximately 2.3–2.7 nm.

The pore structure suggested here is similar to that previous proposed by Gebel and Diat for proton transport in Nafion [48,51]. Gebel and Lambard had previously combined water sorption data with the characteristic dimension from SAXS experiments to predict hydrophilic domain sizes and spacing [51]. The agreement of the water sorption data and Porod analysis from Gebel and co-workers was not very good assuming spherical domains. The fibril structure of hydrophobic cores surrounded by a hydrophobic shell more recently proposed by Gebel and co-workers was more consistent with scattering results and sorption data and we show here it is also consistent with transport data.

The water sorption and hydraulic water transport are not consistent with models that suggest the hydrophilic pores are ~5 nm in diameter [56]. The flow results are also not consistent with the classical Gierke model of spherical clusters connected by narrow channels. If there were narrow channels between large spherical clusters the hydraulic permeability of the pores would be greatly reduced, which would require the spacing between pores to be reduced. The flow rate at fixed pressure increases with the hydraulic radius raised to the 4th power, so a small decrease in channel radius would require more closely spaced hydrophilic channels.

5. Conclusions

Hydraulic permeation of water through Nafion membranes has been examined for different equivalent weights at temperatures 20–80 °C. The principal findings are:

1. Hydraulic permeation decreases with increasing membrane thickness.
2. Hydraulic permeation increases with increasing temperature.
3. Hydraulic permeation increases with decreasing equivalent weight of Nafion.
4. Hydraulic permeation is of negligible importance for water pervaporation; the increase of liquid water activity with pressure is small.
5. Hydraulic permeation is the dominant transport process for water when liquid water is present on both sides of a Nafion membrane.
6. Liquid water removal from the cathode catalyst layer is primarily through the cathode GDL.
7. Water sorption and hydraulic permeation results suggest a hydrophilic pore network in Nafion with hydrophilic domains ~2.5 nm in diameter spaced 5.5 nm apart.

Acknowledgements

This work was supported by the National Science Foundation MRSEC Program through the Princeton Center for Complex Materials NSF DMR-0819860. Q.D. thanks the Chinese Scholarship Council for fellowship support.

References

[1] P.W. Majsztrik, M.B. Satterfield, A.B. Bocarsly, J.B. Benziger, Water sorption, desorption and transport in Nafion membranes, Journal of Membrane Science 301 (2007) 93–106.
[2] B. Kientiz, H. Yamada, N. Nonoyama, A.Z. Weber, Interfacial water transport effects in proton-exchange membranes, Journal of Fuel Cell Science and Technology 8 (2011).
[3] S.H. Ge, X.G. Li, B.L. Yi, I.M. Hsing, Absorption, desorption, and transport of water in polymer electrolyte membranes for fuel cells, Journal of The Electrochemical Society 152 (2005) A1149–A1157.
[4] M. Adachi, T. Navessin, Z. Xie, B. Frisken, S. Holdcroft, Correlation of in situ and ex situ measurements of water permeation through Nafion NRE211 proton exchange membranes, Journal of the Electrochemical Society 156 (2009) B782–B790.
[5] M. Adachi, T. Navessin, Z. Xie, F.H. Li, S. Tanaka, S. Holdcroft, Thickness dependence of water permeation through proton exchange membranes, Journal of Membrane Science 364 (2010) 183–193.
[6] V. Freger, E. Korin, J. Wisniak, E. Korngold, M. Ise, K.D. Kreuer, Diffusion of water and ethanol in ion-exchange membranes: limits of the geometric approach, Journal of Membrane Science 160 (1999) 213–224.
[7] J.T. Hinatsu, M. Mizuhata, H. Takenaka, Water-uptake of perfluorosulfonic acid membranes from liquid water and water-vapor, Journal of The Electrochemical Society 141 (1994) 1493–1498.
[8] C.W. Monroe, T. Romero, W. Merida, M. Eikerling, A vaporization-exchange model for water sorption and flux in Nafion, Journal of Membrane Science 324 (2008) 1–6.
[9] S. Motupally, A.J. Becker, J.W. Weidner, Water transport in polymer electrolyte membrane electrolyzers used to recycle anhydrous HCl. I. Characterization of diffusion and electro-osmotic drag, Journal of The Electrochemical Society 149 (2002) D63–D71.
[10] M.B. Satterfield, J.B. Benziger, Non-fickian water vapor sorption dynamics by Nafion membranes, Journal of Physical Chemistry B 112 (2008) 3693–3704.
[11] T. Takamatsu, M. Hashiyama, A. Eisenberg, Sorption phenomena in Nafion membranes, Journal of Applied Polymer Science 24 (1979) 2199–2220.
[12] S. Tsushima, K. Teranishi, S. Hirai, Water diffusion measurement in fuel-cell SPE membrane by NMR, Energy 30 (2005) 235–245.
[13] A.Z. Weber, J. Newman, Transport in polymer-electrolyte membranes. I. Physical model, Journal of The Electrochemical Society 150 (2003) A1008–A1015.
[14] Q.G. Yan, H. Toghiani, J.X. Wu, Investigation of water transport through membrane in a PEM fuel cell by water balance experiments, Journal of Power Sources 158 (2006) 316–325.
[15] T.A. Zawodzinski, C. Derouin, S. Radzinski, R.J. Sherman, V.T. Smith, T.E. Springer, S. Gottesfeld, Water-uptake by and transport through Nafion(R) 117 membranes, Journal of The Electrochemical Society 140 (1993) 1041–1047.
[16] T.A. Zawodzinski, M. Neeman, L.O. Sillerud, S. Gottesfeld, Determination of water diffusion-coefficients in perfluorosulfonate ionomeric membranes, Journal of Physical Chemistry 95 (1991) 6040–6044.
[17] M.W. Verbrugge, E.W. Schneider, R.S. Conell, R.F. Hill, The effect of temperature on the equilibrium and transport-properties of saturated poly(perfluorosulfonic acid) membranes, Journal of The Electrochemical Society 139 (1992) 3421–3428.
[18] K.A. Mauritz, R.B. Moore, State of understanding of Nafion, Chemical Reviews 104 (2004) 4535–4585.
[19] X. Wu, X. Wang, G. He, J. Benziger, Differences in water sorption and proton conductivity between Nafion and SPEEK, Journal of Polymer Science Part B: Polymer Physics 49 (2011) 1437–1445.
[20] Q. Zhao, P. Majsztrik, J. Benziger, Diffusion and interfacial transport of water in Nafion, Journal of Physical Chemistry B 115 (2011) 2717–2727.
[21] J. Peron, A. Mani, X.S. Zhao, D. Edwards, M. Adachi, T. Soboleva, Z.Q. Shi, Z. Xie, T. Navessin, S. Holdcroft, Properties of Nafion (R) NR-211 membranes for PEMFCs, Journal of Membrane Science 356 (2010) 44–51.
[22] R.A. Register, T.R. Bell, Miscible blends of zinc-neutralized sulfonated polystyrene and poly(2,6-dimethyl 1,4-phenylene oxide), Journal of Polymer Science Part B: Polymer Physics 30 (1992) 569–575.
[23] C. Yang, S. Srinivasan, A.B. Bocarsly, S. Tulyani, J.B. Benziger, A comparison of physical properties and fuel cell performance of Nafion and zirconium phosphate/Nafion composite membranes, Journal of Membrane Science 237 (2004) 145–161.
[24] G. Gebel, O. Diat, Neutron and X-ray scattering: suitable tools for studying ionomer membranes, Fuel Cells 5 (2005) 261–276.
[25] K.A. Page, F.A. Landis, A.K. Phillips, R.B. Moore, SAXS analysis of the thermal relaxation of anisotropic morphologies in oriented Nafion membranes, Macromolecules 39 (2006) 3939–3946.
[26] L. Rubatat, O. Diat, Stretching effect on Nafion fibrillar nanostructure, Macromolecules 40 (2007) 9455–9462.
[27] M. Pineri, G. Gebel, R.J. Davies, O. Diat, Water sorption–desorption in Nafion (R) membranes at low temperature, probed by micro X-ray diffraction, Journal of Power Sources 172 (2007) 587–596.
[28] M. Eikerling, Y.I. Kharkats, A.A. Kornyshev, Y.M. Volfkovich, Phenomenological theory of electro-osmotic effect and water management in polymer electrolyte proton-conducting membranes, Journal of the Electrochemical Society 145 (1998) 2684–2699.
[29] J. Divisek, M. Eikerling, V. Mazin, H. Schmitz, U. Stimming, Y.M. Volfkovich, A study of capillary porous structure and sorption properties of Nafion proton-exchange membranes swollen in water, Journal of The Electrochemical Society 145 (1998) 2677–2683.
[30] M. Eikerling, A.A. Kornyshev, U. Stimming, Electrophysical properties of polymer electrolyte membranes: a random network model, Journal of Physical Chemistry B 101 (1997) 10807–10820.
[31] M.H. Eikerling, P. Berg, Poroelectroelastic theory of water sorption and swelling in polymer electrolyte membranes, Soft Matter 7 (2011) 5976–5990.
[32] P. Majsztrik, A. Bocarsly, J. Benziger, Water permeation through nafion membranes: the role of water activity, Journal of Physical Chemistry B 112 (2008) 16280–16289.
[33] M. Adachi, T. Navessin, Z. Xie, S. Holdcroft, POLY 364-Ex-situ water permeation measurements through proton exchange membranes, Abstracts of Papers of the American Chemical Society 238 (2009).
[34] P.W. Majsztrik, A.B. Bocarsly, J.B. Benziger, Viscoelastic response of nafion. effects of temperature and hydration on tensile creep, Macromolecules 41 (2008) 9849–9862.
[35] M.B. Satterfield, J.B. Benziger, Viscoelastic properties of nafion at elevated temperature and humidity, Journal of Polymer Science Part B: Polymer Physics 47 (2009) 11–24.
[36] G. Gebel, O. Diat, S. Escribano, R. Mosdale, Water profile determination in a running PEMFC by small-angle neutron scattering, Journal of Power Sources 179 (2008) 132–139.
[37] G. Gebel, S. Lyonnard, H. Mendil-Jakani, A. Morin, The kinetics of water sorption in Nafion membranes: a small-angle neutron scattering study, Journal of Physics-Condensed Matter 23 (2011).
[38] Z. Zhang, A.E. Marble, B. MacMillan, K. Promislow, J. Martin, H. Wang, B.J. Balcom, Spatial and temporal mapping of water content across Nafion membranes under wetting and drying conditions, Journal of Magnetic Resonance 194 (2008) 245–253.
[39] Z. Zhang, K. Promislow, J. Martin, H. Wang, B.J. Balcom, Bi-modal water transport behavior across a simple Nafion membrane, Journal of Power Sources 196 (2011) 8525–8530.
[40] S.K. Park, E.A. Cho, I.H. Oh, Characteristics of membrane humidifiers for polymer electrolyte membrane fuel cells, Korean Journal of Chemical Engineering 22 (2005) 877–881.
[41] Perma Pure LLC, http://www.permapure.com/industry/enviro/technology/, 2011.
[42] Cell Craft, http://www.cellkraft.se/humidity_and_steam/home.html, 2011.
[43] J. Benziger, J. Nehlsen, D. Blackwell, T. Brennan, J. Itescu, Water flow in the gas diffusion layer of PEM fuel cells, Journal of Membrane Science 261 (2005) 98–106.
[44] T.D. Gierke, W.Y. Hsu, The cluster-network model of ion clustering in perfluorosulfonated membranes, ACS Symposium Series 180 (1982) 283–307.
[45] T.D. Gierke, G.E. Munn, F.C. Wilson, The morphology in Nafion perfluorinated membrane products, as determined by wide-angle and small-angle X-ray studies, Journal of Polymer Science Part B: Polymer Physics 19 (1981) 1687–1704.
[46] T.D. Gierke, G.E. Munn, F.C. Wilson, Morphology of perfluorosulfonated membrane products – wide-angle and small-angle X-ray studies, ACS Symposium Series 180 (1982) 195–216.
[47] A. Eisenberg, Clustering of ions in organic polymers. A theoretical approach, Macromolecules 3 (1970) 147–154.
[48] O. Diat, G. Gebel, Proton channels, Nature Materials 7 (2008) 13–14.
[49] G. Gebel, P. Aldebert, M. Pineri, Swelling study of perfluorosulphonated ionomer membranes, Polymer 34 (1993) 333–339.
[50] G. Gebel, Structural evolution of water swollen perfluorosulfonated ionomers from dry membrane to solution, Polymer 41 (2000) 5829–5838.
[51] G. Gebel, J. Lambard, Small-angle scattering study of water-swollen perfluorinated ionomer membranes, Macromolecules 30 (1997) 7914–7920.
[52] K.D. Kreuer, On the development of proton conducting polymer membranes for hydrogen and methanol fuel cells, Journal of Membrane Science 185 (2001) 29–39.
[53] M. Pineri, A. Eisenberg, Structure and properties of ionomers, in: NATO ASI Series. Series C: Mathematical and Physical Sciences, Reidel Pub. Co., Norwell, MA, 1987.
[54] K. Schmidt-Rohr, Q. Chen, Parallel cylindrical water nanochannels in Nafion fuel-cell membranes, Nature Materials 7 (2008) 75–83.
[55] M. Fujimura, T. Hashimoto, H. Kawai, Small-angle X-ray-scattering study of perfluorinated ionomer membranes. 1. Origin of 2 scattering maxima, Macromolecules 14 (1981) 1309–1315.
[56] M. Fujimura, T. Hashimoto, H. Kawai, Small-angle X-ray-scattering study of perfluorinated ionomer membranes. 2. Models for ionic scattering maximum, Macromolecules 15 (1982) 136–144.
[57] K. Daly, Structure and Properties of Nafion from Molecular Simulations, Princeton University, Princeton, NJ, 2011.
[58] R.B. Bird, W.E. Stewart, E.N. Lightfoot, Transport Phenomena, 2nd ed., Wiley, New York, 2002.